Sustainable Polymer & Energy

SCIEPublish

Article

Step-Growth Copolymerization of Cyclic and Acyclic Perfluoroolefins with Bisphenols

Erfan Masaeli [1], Maxim E. Solovyev [1], Gustavo Muñoz [1], William W. Johnson [1], Elnaz Janghorban [2], Giovanni Octavio Martinez Ortega [1], Charles U. Pittman, Jr. [1] and Dennis W. Smith, Jr. [1,*]

[1] Department of Chemistry, Mississippi State University, Mississippi State, MS 39762, USA; sm3892@msstate.edu (E.M.); ms4445@msstate.edu (M.E.S.); gam318@msstate.edu (G.M.); wwj38@msstate.edu (W.W.J.); gm1103@msstate.edu (G.O.M.O.); cpittman@chemistry.msstate.edu (C.U.P.J.)

[2] Department of Sustainable Bioproducts, Mississippi State University, Starkville, MS 39759, USA; ej646@msstate.edu (E.J.)

* Corresponding author. E-mail: dsmith@chemistry.msstate.edu (D.W.S.J.)

Received: 22 July 2026; Revised: 6 August 2026; Accepted: 22 September 2026; Available online: 12 October 2026

ABSTRACT: Base-initiated copolymerization of bisphenols with cyclic and acyclic perfluoroolefins was investigated as an extension of addition–elimination polymerization toward compositionally variable feedstocks that model (per-and polyfluoroalkyl substances) PFAS waste. Perfluoro-4-methylpent-2-ene (PFP), perfluorohept-1-ene (PFH), perfluorocyclohexene (PFCH), and perfluorocyclopentene (PFCP) were paired in selected combinations and reacted in the presence of bisphenol-A (BPA) and bisphenol-AF (BPF), respectively, under basic conditions to generate a series of semi-fluorinated copolymers. These reactions yielded copolymers containing fluorinated segments derived from both cyclic and acyclic olefin comonomers. Structural incorporation and copolymer compositions were evaluated by nuclear magnetic resonance and infrared spectroscopy, while molecular mass and thermal behavior were examined by gel permeation chromatography, differential scanning calorimetry, and thermogravimetric analysis. The resulting copolymers exhibited broad compositional and thermal variability while retaining unsaturated fluorinated sites capable of further reaction, such as capable of further thermal reactivity. These results establish structurally distinct perfluoroolefins as model fluorinated feedstocks for investigating addition–elimination polymerization and provide a foundation for future studies using more compositionally complex fluorinated feedstocks.

Keywords: Fluoropolymers; PFAS derivatives; Perfluoro cycloolefin copolymerization; Addition–elimination chemistry; Bisphenols; Thermal reactivity

1. Introduction

Fluorinated polymers occupy an important position among high-performance materials, as they combine chemical resistance, thermal stability, low surface energy, low moisture uptake, and low dielectric constants in ways that are inconceivable to replicate with hydrocarbon-based polymers [1]. These properties are commonly associated with the strength and low polarizability of carbon–fluorine bonds. However, fluoropolymer performance is not controlled by fluorine content alone. Backbone architecture, segmental rigidity, fluorinated-unit placement, aromatic content, and residual reactive functionality all influence

© 2026 The authors. This is an open access article under the Creative Commons Attribution 4.0 International License (https://creativecommons.org/licenses/by/4.0/).

solubility, processability, glass-transition behavior, thermal response, and network formation [2,3]. As a result, modern fluoropolymer synthesis increasingly depends on methods that can incorporate fluorinated structures into macromolecules with chemical precision rather than simply increasing the overall fluorine fraction. Most established fluoropolymers are prepared by the chain-growth polymerization of fluorinated olefins, including systems based on tetrafluoroethylene, vinylidene fluoride, hexafluoropropylene, and related monomers [4]. These methods produce many commercial materials with properties demanded for chemical [5], electronic [1,3], aerospace [6], energy [7], coating [8], and membrane applications [9]. Recent developments in fluoro-functionalized polyether electrolytes further demonstrate the importance of controlled fluorination in advanced polymer materials for energy storage applications [10].

Nevertheless, chain-growth polymerization is not equally suitable for all fluorinated olefins. Highly substituted perfluoroalkenes [11], cyclic perfluoroolefins [12], and structurally diverse fluorinated feedstocks may present challenges related to reactivity, steric demand, regioselectivity, and uncontrolled side reactions [13]. These limitations become particularly important when the goal is to optimize and limit valuable fluorocarbon content and to produce semi-fluorinated materials with robust (by hydrocarbon standards) bisphenol-derived aromatic ether content without sacrificing extreme properties granted by perfluorinated repeating units.

Step-growth addition–elimination chemistry provides a complementary strategy for incorporating electron-deficient perfluorinated olefins into polymer backbones. Utilizing this approach, phenoxide nucleophiles add to a fluorinated alkene, followed by fluoride elimination to regenerate an unsaturated fluorinated alkene [14]. This mechanism is distinct from radical fluoroolefin polymerization as step-growth is governed by nucleophilic substitution chemistry rather than radical propagation [4]. The outcome depends strongly on fluoroolefin electrophilicity [15], phenoxide nucleophilicity [16], accessibility of vinylic [17] or allylic fluorine atoms [16], and the stability of the substituted alkene products. This is a powerful synthetic tool for the polymerization of fluoroolefins, as it can undergo vinylic or allylic fluoride elimination depending on the monomer structure, and the regenerated unsaturation can remain available for additional substitution. Consequently, addition–elimination polymerization may produce linear chains, branched macromolecules, gel fractions, and thermally curable network precursors [14,18,19]. Reaction conditions such as base strength, temperature, monomer ratio, order of addition, and bisphenol identity therefore play a central role in controlling molecular-mass growth, branching, and crosslinking [20–22]. This provides many synthetic controls in the design of processable fluorinated pre-network materials with latent curing capability [23].

Our labs have developed a broad foundation for this type of fluorinated step-growth chemistry [21,24,25]. Earlier studies demonstrated that bis (trifluorovinyl) aromatic ethers [22,26], octafluorocyclopentene [6,27], decafluorocyclohexene [12], and related perfluorocycloalkenyl monomers can react with bisphenols to produce semi-fluorinated polymers with useful thermal stability, film-forming behavior, and tunable structures [13,14,26,28–30]. These reports established that cyclic perfluoroolefins are not merely inert fluorocarbon fragments, but reactive electrophilic building blocks whose substitution behavior can be directed through nucleophilic addition–elimination chemistry [18,31,32]. More recently, our group has extended this platform from cyclic perfluoroolefin systems to acyclic perfluoroalkenes as model PFAS waste-relevant feedstocks. In that study, perfluoro-4-methylpent-2-ene (PFP) and perfluorohept-1-ene (PFH) were reacted with bisphenol-A (BPA) and bisphenol-AF (BPF) under basic conditions to form unsaturated semi-fluorinated polymeric materials [14,17]. PFP was selected as a highly substituted acyclic perfluoroolefin derived from hexafluoropropylene dimerization, while PFH is relevant as the terminal perfluoroolefin obtainable from perfluorooctanoic acid (PFOA) decarboxylation. These monomer origins and their relationship to fluorinated feedstock valorization are shown schematically in Figure 1. Although these monomers do not represent the full complexity of real PFAS waste streams, they

provide a practical platform for evaluating proof-of-concept reactivity in fluorinated feedstock upcycling. The previous PFP/PFH study established several important features of acyclic perfluoroolefin addition–elimination polymerization. PFP reacted readily and showed a strong tendency toward branching and gelation, whereas PFH required increased temperatures and introduced longer perfluoroalkyl segments that influenced thermal behavior [14]. That work primarily established the homopolymerization behavior of PFP and PFH with bisphenols and included an initial example of a PFP/PFH/BPF copolymer. The observation that two distinct acyclic perfluoroolefins could be incorporated into a common polymeric product.

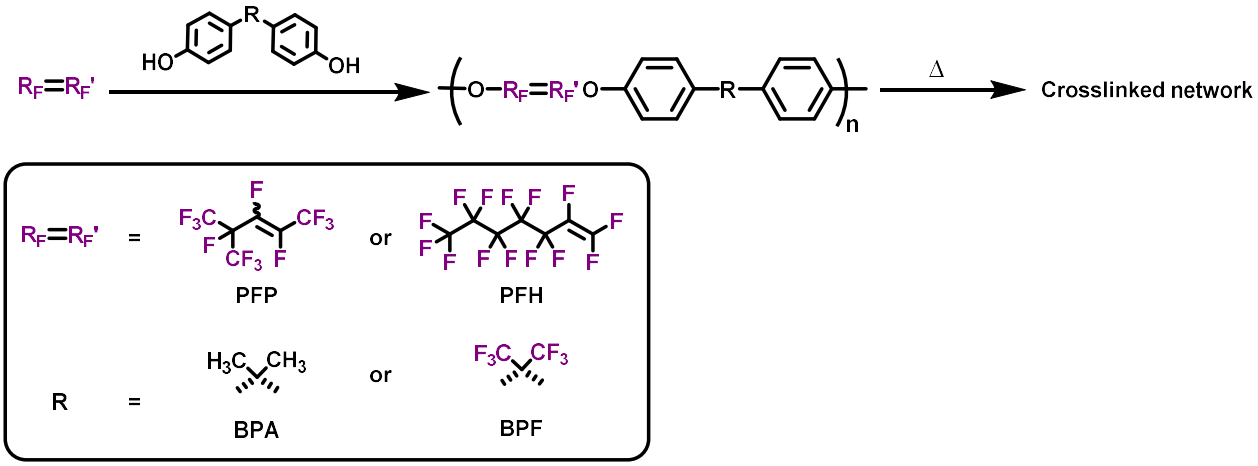


Figure 1. Previous study scheme featuring polymerization of acyclic perfluoroolefins with aromatic bisphenols [14].

This present work builds directly on the previous PFP/PFH study and expands the scope of perfluoroolefin addition–elimination copolymerization from individual fluorolefin homopolymerization and initial acyclic copolymerization to broader binary comonomer systems. Here, PFP, PFH, perfluorocyclohexene (PFCH), and perfluorocyclopentene (PFCP) were reacted with BPA and BPF to compare the formation and measure the properties of the isolated THF-soluble products to determine how olefin geometry, substitution pattern, electrophilicity, and bisphenol structure influence copolymer formation, relative molecular mass, and thermal properties. The central hypothesis is that cyclic and acyclic perfluoroolefins can be incorporated via a shared bisphenol-based addition–elimination pathway to yield stable unsaturated semi-fluorinated copolymers with distinct and potentially valuable properties. This series provides a foundation for future studies of fluorinated-feedstock valorization [14]. Our current study establishes comonomer selection as a practical strategy to expand perfluoroolefin addition–elimination polymer chemistry toward compositionally tunable unsaturated, semi-fluorinated copolymer platforms.

2. Materials and Methods

2.1. Materials

Perfluoro-4-methylpent-2-ene (PFP) (1), perfluorohept-1-ene (PFH) (2), octafluorocyclopentene (PFCP) (3), and decafluorocyclohex-1-ene (PFCH) (4) were purchased from SynQuest Laboratories Inc. (Alachua, Fl, USA) and used as model perfluoroolefin feedstocks. Bisphenol-A (BPA) was purchased from Alfa Aesar (Ward Hill, MA, USA), and bisphenol-AF (BPF) was obtained from AK Scientific (Union City, CA, USA). Prior to use, both bisphenols were recrystallized from a 1:1 acetic acid/water mixture. Anhydrous *N,N*-dimethylformamide (DMF, 99.8%, extra dry over molecular sieves) was supplied by Thermo Fisher Scientific (Waltham, MA, USA). Anhydrous triethylamine (Et_3N) was obtained from Carolina Chemical (Burlington, NC, USA). Methanol (99.8%) was purchased from Oakwood Chemical Inc. (Estill, SC, USA), and HPLC-grade tetrahydrofuran (THF >99.9%) was supplied by Fisher Scientific

(Pittsburgh, PA, USA). Unless otherwise stated, all reagents and solvents were used as received without further purification.

2.2. Characterization

Attenuated total reflectance Fourier transform infrared spectroscopy (ATR-FTIR) was performed using a Thermo Scientific™ (Waltham, MA, USA) Nicolet™ iS™5 FT-IR spectrometer. Spectra were recorded from 500 to 4500 cm^{-1} using 16 scans, a spectral resolution of 4 cm^{-1}, and a data spacing of 0.482 cm^{-1}. Nuclear magnetic resonance (NMR) spectroscopy was carried out on a Bruker Avance III spectrometer (Billerica, MA, USA). ^{1}H NMR spectra were collected at 500 MHz, and ^{19}F NMR spectra were collected at 470 MHz using $CDCl_3$ as the solvent at 298 K. Relative perfluoroolefin compositions were estimated from selected diagnostic ^{19}F NMR integrations after normalization for the number of fluorine nuclei represented by each resonance:

$$X_1(\%) = \frac{I_1}{I_1 + I_2} \times 100\%$$

X_1 is the fractional composition of one of the comonomers. I_1 is the integration of the combined signals of one of the comonomers in the resulting copolymers, and I_2 another combination of comonomers. As the polymer spectra contain broad and partially overlapping resonances, the reported compositions are considered NMR-based estimates.

Thermogravimetric analysis (TGA) was conducted on a TA Instruments Discovery TGA 5500 (New Castle, DE, USA) under both nitrogen and air atmospheres at a gas flow rate of 20 mL/min. Samples were heated at a rate of 10 °C/min. Differential scanning calorimetry (DSC) was performed using a TA Instruments Discovery DSC 250 (New Castle, DE, USA) under nitrogen at a flow rate of 20 mL/min and a heating rate of 10 °C/min. Gel permeation chromatography (GPC) measurements were performed on an ACQUITY Advanced Polymer Chromatography (APC) (Milford, MA, USA) system using THF as the eluent at a flow rate of 1.0 mL/min and an operating temperature of 35 °C. An OMNISEC REVEAL multidetector system from Malvern Panalytical (Westborough, MA, USA) was used at 35 °C. Polymer samples were prepared as THF solutions with concentrations of 1–5 mg/mL and filtered through Cole-Parmer PTFE syringe filters with a 25 mm diameter and 0.2 µm pore size prior to injection. Number-average molar mass (M_n) and Mass-average molar mass (M_w) values were calculated using conventional calibration against polystyrene standards. As the molecular masses within equivalent hydrodynamic volumes of the fluorinated polymers described in this work are expected to differ from those of polystyrene standards, the reported molecular masses are considered relative to polystyrene calibration [14].

2.3. Polymerization

Initial screening reactions were performed until insoluble fractions were observed at 24 h reaction time for all combinations. To investigate the scope of reactivity, all reactions showcased as part of this study are from 23 h reactions where the products had no measurable THF-insoluble fraction observed. The present study focuses on processable copolymer precursors suitable for solution-state characterization; corresponding preparative reactions were repeated under identical conditions and terminated after 23 h. This one-hour adjustment was selected empirically to limit late-stage network formation and improve recovery of the soluble copolymer fraction.

2.3.1. Copolymerization of PFP and PFH with BPA [***Poly(1-co-2)A***]

To a dry 10 mL glass reaction tube equipped with a magnetic stir bar under a nitrogen at 30 °C was added under dry conditions, triethylamine (Et_3N, 0.56 mL, 4 mmol), *N,N*-dimethylformamide (DMF, 1 mL),

and bisphenol-A (BPA, 456.6 mg, 2 mmol), followed by a solution of (PFH, 203.5 μL, 1 mmol) in dry DMF (1 mL). The reaction mixture was warmed to 30 °C and maintained at this temperature for 20 min, and PFP (187.5 μL, 1 mmol) was then added dropwise, and the reaction mixture was stirred at 60 °C. The reaction was subsequently repeated under identical conditions and terminated after 23 h to prevent further network formation. The product was precipitated into methanol (150 mL), collected by filtration, washed thoroughly with methanol, and dried overnight under reduced pressure at 60 °C. The THF-soluble fraction obtained from the 23 h preparative reaction was isolated by decantation, followed by solvent removal, and gave a white powder in 84% yield. IR ν = 1504 (m; C=C), 1164 (b; –CF_3), 1002 (m; C–F), 831 (m; –CF_3). ^{1}H NMR (500 MHz, $CDCl_3$, δ): 6.6–7.3 (m; Ar–H), 1.6 (m; Ar–$C(CH_3)_2$–Ar′). ^{19}F NMR (470 MHz, $CDCl_3$, δ): −55.7 to −63.9 (m; R=C(F)(**CF_3**)**$_2$**), −70.4 (m; –O–**CF_2**), −77.6 (m; C(**CF_3**)(R)(R′)–C(F)=$C(CF_3)_2$), −80.9 to −86.5 (m; –$(CF_2)_4$–**CF_3** and –$(CF_2)_3$–**CF_3**), −106.6 (m; –O–(R)C=C(**F**)–O–), −111.0 to −127.5 (m; adjacent –**CF_2**–), −154.2 (m; (R)(R′)C=C(**F**)(R″)). See Table 1 for molecular masses and thermal characterization.

2.3.2. Copolymerization of PFP and PFCH with BPA [***Poly(1-co-4)A***]

As described similarly above, PFCH (160 μL, 1.0 mmol) and PFP (187.5 μL, 1 mmol) were copolymerized under identical reaction conditions. The reaction was subsequently repeated under otherwise identical conditions and terminated after 23 h to limit further network formation and improve recovery of the soluble fraction. The THF-soluble product obtained from the 23 h preparative reaction was used for the characterization reported in this study. This product is a yellow powder in 75% yield. IR ν = 1410 (w; C=C), 1231 (m; –CF_3), 713 (s; –CF_3). ^{1}H NMR (500 MHz, $CDCl_3$, δ): 6.5–7.5 (m; Ar–H), 1.7 (m; Ar–$C(CH_3)_2$–Ar′). ^{19}F NMR (470 MHz, $CDCl_3$, δ): −54.8 to −64.2 (m; R–C=C(**CF_3)$_2$**), −72.8 (m; −C(R)−O−C(**F**)(C(R′))), −77.5 to −83.5 (m;R(**CF_3**)(R′)C(F)=C(**CF_3**)$_2$), −106.0 to −112.7 (m; allylic PFCH-derived products), −114.6 (s; –R–O–CF_2–**$(CF_2)_2$**–CF_2–O–R–), −115.3 (m; –R–O–C(F)–CF_2–**CF_2**–$(CF_2)_2$–), −117.1 (m; R–O–CF_2–**CF_2**–$(CF_2)_2$–C(F)), −125.4 (m; –R–O–**CF_2**–$(CF_2)_2$–CF_2–O–R–), −133.4 (m; R–O–**CF_2–**$(CF_2)_2$–**CF_2–**C(F)), −143.4 (m; R–O–C(**F**)(R)–C(R′)). See Table 1 for other characterization.

2.3.3. Copolymerization of PFH and PFCH with BPA [***Poly(2-co-4)A***]

As described similarly above, PFH (203.5 μL, 1.0 mmol) and PFCH (160 μL, 1.0 mmol) were copolymerized. The reaction was subsequently repeated under otherwise identical conditions and terminated after 23 h to limit further network formation. The THF-soluble fraction obtained from the 23 h preparative reaction was an orange solid in 80% yield and used for the characterization reported in this study. IR ν = 1421 (m; C=C) , 1264 (m; –CF_3), 897 (w; C–F), 752 (s; –CF_3). ^{1}H NMR (500 MHz, $CDCl_3$, δ): 6.5–7.5 (m; Ar–H), 1.6–1.9 (m; Ar–$C(CH_3)_2$–Ar′). ^{19}F NMR (470 MHz, $CDCl_3$, δ): −78.8 to −86.0 (m; –$(CF_2)_4$–**CF_3**), −109.6 (m; –O–(R)C=C(**F**)–O–), −117.4 (m; R–O–CF_2–**CF_2**–C(R′)), −115.2 (m; O–CF_2–**CF_2**–C(R′)–O–), −115.8 to −128.8 (m; adjacent **CF_2** groups), −133.2 (m; –O–**CF_2**–CF_2–C(R′)–O–, and R–O–**CF_2**–$(CF_2)_4$–**CF_2**–C(F)), −140.0 to −155.5 (m; other substituted vinylic –**F** nuclei). See Table 1 for molecular masses and thermal characterization.

2.3.4. Copolymerization of PFH and PFCH with BPF [***Poly(2-co-4)AF***]

To a dry 10 mL glass reaction tube equipped with a magnetic stir bar under nitrogen at 30 °C, triethylamine (Et_3N, 0.56 mL, 4 mmol), dry DMF (1 mL), and bisphenol-AF (BPF, 672 mg, 2 mmol) were added, followed by a mixture of PFH (203.5 μL, 1 mmol) in dry DMF (1 mL). The reaction mixture was warmed to 30 °C and stirred for 20 min. PFCH (160 μL,1 mmol) was then added dropwise, and the reaction mixture was stirred at 60 °C for 23 h. The reaction mixture was precipitated in methanol (150 mL), filtered, thoroughly washed with methanol, and dried overnight under vacuum at 60 °C. The isolated THF-soluble product was a dark orange solid in 90% yield. IRν = 1508 (m; C=C), 1157 (b; –CF_3), 991–1013 (m; C–F),

814 (m; –CF_3). ^{1}H NMR (500 MHz, $CDCl_3$, δ): 6.5–7.5 (m; Ar–H). ^{19}F NMR (470 MHz, $CDCl_3$, δ): −64.2 (s; Ar−**C(CF₃)₂**−Ar′), −78.8 to −86.0 (m; –$(CF_2)_4$–**CF_3**), −109.6 (m; –O–(R)C=C(**F**)–O–), −115.8 to −128.8 (m; adjacent **CF_2** groups), −133.2 (m; –O–**CF_2**–CF_2–C(R′)–O–), −140.0 to −155.5 (m; other substituted vinylic –**F** nuclei). See Table 1 for molecular masses and thermal characterization.

2.3.5. Copolymerization of PFP and PFCH with BPF [*Poly(1-co-4)AF*]

For the synthesis of ***poly(1-co-4)AF*** products, the same copolymerization procedure was used as in ***poly(1-co-4)A***. PFP (187.5 µL, 1 mmol) and PFCH (160 µL, 1.0 mmol) were copolymerized under identical reaction conditions. This reaction was stirred at room temperature (30 °C) for 12 h, then heated to 60 °C and stirred for 23 h. The THF-soluble fraction was a dark yellow powder in 87% yield. It was isolated from the 23 h preparative reaction by decantation and removal of THF under reduced pressure at 60 °C and used for the characterization reported in this study. IRν = 1509 (m; C=C), 1168 (b; –CF_3), 1000 (m; C–F), 829 (m; –CF_3). ^{1}H NMR (500 MHz, $CDCl_3$, δ): 6.5–7.5 (m; Ar–H), 1.60–1.86 (m; Ar–$C(CH_3)_2$Ar′).^{19}F NMR (470 MHz, $CDCl_3$, δ): −54.7 to −61.0 (m; R=C(F)(**CF_3**)$_2$), −64.3 (s; Ar−**C(CF₃)₂**−Ar), −72.8 (m; −RO−C(**F**)=$(CF_3)_2$−), −77.0 to −84.0 (m; C(**CF_3**)(R)(R′)−C(F)=$C(CF_3)_2$), −106.5 to −112.8 (m; trace allylic fluorinated products), −114.4 to −120.2 (m; −O−**CF_2**−$(CF_2)_2$−C(R′)−O−, −O−$(CF_2)_2$−**CF_2**−C(R′)−O−, and adjacent cyclic −CF_2− groups), −123.4 (m; −O−C(R)−**CF_2**−C(R′)−O−),−124.5 (m; −C(F)=C(F)−C(F)(OAr)−C(R)−, −C(R′)−C(F)=C(**F**)(OAr)−C(R)−), −127.0 (m; −O−C(R)=C(F)−CF_2−**CF_2**−), −129.8 (m; C(R′)−CF_2−CF_2−CF_2−C(F)(OAr)), −133.3 (m; −C(F)−CF_2−$C(CF_2)$−$C(CF_2)$−CF_2−C(OAr)−), −134.5 (m; −CF_2−**CF_2**−CF_2−C(F)=C(F)(OAr)), −135.0 (m;−O−C(R)=C(F)−**CF_2**−CF_2−), −141.0 (m; −C(OAr)(F)−C(F)=C(F)−CF_2−C(R)), −144.1 (m;−C(F)=C(**F**)−C(F)(OAr)−C(R)), −153.2 (m; −C(OAr)(F)−C(F)=C(**F**)−CF_2−C(R)). See Table 1 for other characterizations.

2.3.6. Copolymerization of PFP and PFCP with BPF [*Poly(1-co-3)AF*]

To a dry 10 mL glass reaction tube equipped with a magnetic stir bar, under a nitrogen at 30 °C, was added triethylamine (Et_3N, 0.56 mL, 4 mmol), dry DMF (1 mL), and bisphenol-AF (BPF, 672 mg, 2 mmol), followed by a solution of PFCP (135 µL, 1 mmol) in dry DMF (1 mL). The reaction mixture was cooled to 0–20 °C and maintained at this temperature for 20 min. PFP (187.5 µL, 1 mmol) was then added dropwise, and the reaction mixture was stirred at 25 °C for 23 h. The reaction mixture was poured into methanol (150 mL), and the precipitated product was collected by filtration, washed thoroughly with methanol, and dried overnight under vacuum at 60 °C. The reaction was subsequently terminated after 23 h to limit further network formation. The THF-soluble fraction obtained from the 23 h preparative reaction was a white solid in 92% yield. by decantation and removal of THF under reduced pressure and was used for the characterization reported in this study. IRν = 1509 (m; C=C), 1168 (b; –CF_3), 968 (m; C–F), 828 (m; –CF_3). ^{1}H NMR (500 MHz, $CDCl_3$, δ): 6.5–7.5 (m; Ar–H), 1.6–1.9 (m; Ar–$C(CH_3)_2$–Ar′). ^{19}F NMR (470 MHz, $CDCl_3$, δ): −59.8 (m; R=C(F)(**CF_3**)$_2$), −64.3 (s; Ar−**C(CF₃)₂**−Ar′), −73.4 (m; −O−C(**F**)(CF_3)−), −78.8 to −86.4 (m; allylic −**CF_3** groups), −109.9 to −117.8 (m; –O–$(CF_2)_2$–**CF_2**), −133.5 (m; –O–**$(CF_2)_2$**–CF_2), −141.1 to −150.9 (m; other substituted vinylic −**F** nuclei). See Table 1 for other characterizations.

Table 1. Summarized data of ***poly(x-co-y)A/AF*** copolymers with fixed olefin feed ratio (1:1).

Copolymer/Property	M_n [(a)] (kDa)	M_w (kDa)	PDI	Olefin Ratio (%) [(b)] x:y	T_g (°C) [(c)]	$T_{d5\%}$ (°C) [(d)]	
						In N_2	In Air
poly(1-co-2)A	13.2	17.2	1.3	23:77	114	262.3	378.5
poly(1-co-4)A	13.1	23.8	1.9	59:41	125	243.7	366.0
poly(2-co-4)A	15.2	17.0	1.1	57:43	131	363.0	310.8
poly(2-co-4)AF	13.4	20.3	1.5	47:53	201	406.0	362.5
poly(1-co-4)AF	16.2	17.4	1.1	35:65	123	408.6	397.1
poly(1-co-3)AF	13.0	16.3	1.3	34:66	116	418.4	394.7

(a) By GPC in THF at 35 °C *vs.* Polystyrene standards. (b) Olefin ratio by ^{19}F NMR in $CDCl_3$. (c) DSC, 10 °C/min in nitrogen (2nd cycle). (d) TGA, 10 °C/min.

3. Results and Discussion

3.1. General Strategy for Perfluoroolefin Addition–Elimination Copolymerization

The present study extends bisphenol-based addition–elimination polymerization from single-perfluoroolefin systems to binary comonomer systems composed of structurally distinct cyclic and acyclic fluorinated olefins. In addition to tailored high-performance properties depending on fluorocarbon content, tuning copolymer composition with high free volume perfluorocycloolefins will also affect permeability and selectivity for separation membrane applications [1]. As summarized in Figure 2, perfluoro-4-methylpent-2-ene (PFP) (1), perfluorohept-1-ene (PFH) (2), perfluorocyclopentene (PFCP) (3), and perfluorocyclohexene (PFCH) (4) were combined in selected binary pairings and reacted with either bisphenol-A (BPA) or bisphenol-AF (BPF) under triethylamine-mediated conditions. All mixed-perfluoroolefin polymerizations employed a 2:1:1 molar feed ratio of bisphenol, perfluoroolefin 1, and perfluoroolefin 2 (2.0 mmol:1.0 mmol:1.0 mmol). The products are designated using the ***poly(x-co-y)A/AF*** notation, where x and y identify the two perfluoroolefin comonomers and the suffix A or AF denotes the BPA- or BPF-derived system, respectively. The full monomer compositions and product designations are summarized in Figure 2.

The structures presented in Figure 2 are idealized representations of the THF-soluble copolymer and should not be interpreted as single, perfectly defined repeating units. This distinction is important because addition–elimination polymerization of perfluoroolefins can generate multiple substituted alkene environments during chain growth. Each incorporated perfluoroolefin unit may retain residual unsaturation and remain susceptible to additional nucleophilic substitution. Consequently, the isolated materials are expected to contain distributions of linear and branched structures rather than one uniform macromolecular architecture. Nevertheless, the idealized structures provide a useful framework for comparing how comonomer identity, cyclic versus acyclic olefin structure, and bisphenol selection influence copolymer formation.

The mechanistic basis for this chemistry involves nucleophilic addition and elimination of a fluorine atom from the carbon to which the nucleophile is added or from allylic fluorine atoms. Subsequent addition-elimination can result in linear or branching polymers, as illustrated in Figure S1 using PFH as a

representative acyclic perfluoroolefin. Under basic conditions, the bisphenol is converted to a phenoxide-containing species that can add to the electron-deficient fluoroalkene. The resulting fluorinated carbanion intermediate undergoes fluoride elimination to regenerate an unsaturated fluorinated unit. This first addition–elimination event provides mono-substituted PFH-derived structures that can undergo further polymerization or termination with subsequent phenoxide or fluoroolefin groups. Depending on the position of fluoride elimination, the reaction can proceed through vinylic or allylic pathways, producing substitution motifs with different regiochemical fluorine environments. As shown above, variable regioisomers and multiple substitutions promote branching and network formation, the relative rates of which determine copolymer architecture, rheological properties, and reactivity to crosslinking. Consequently, solid networks can be produced (with or without other reactive components), giving tunable crosslink densities and, potentially, a wide range of thermoset products.

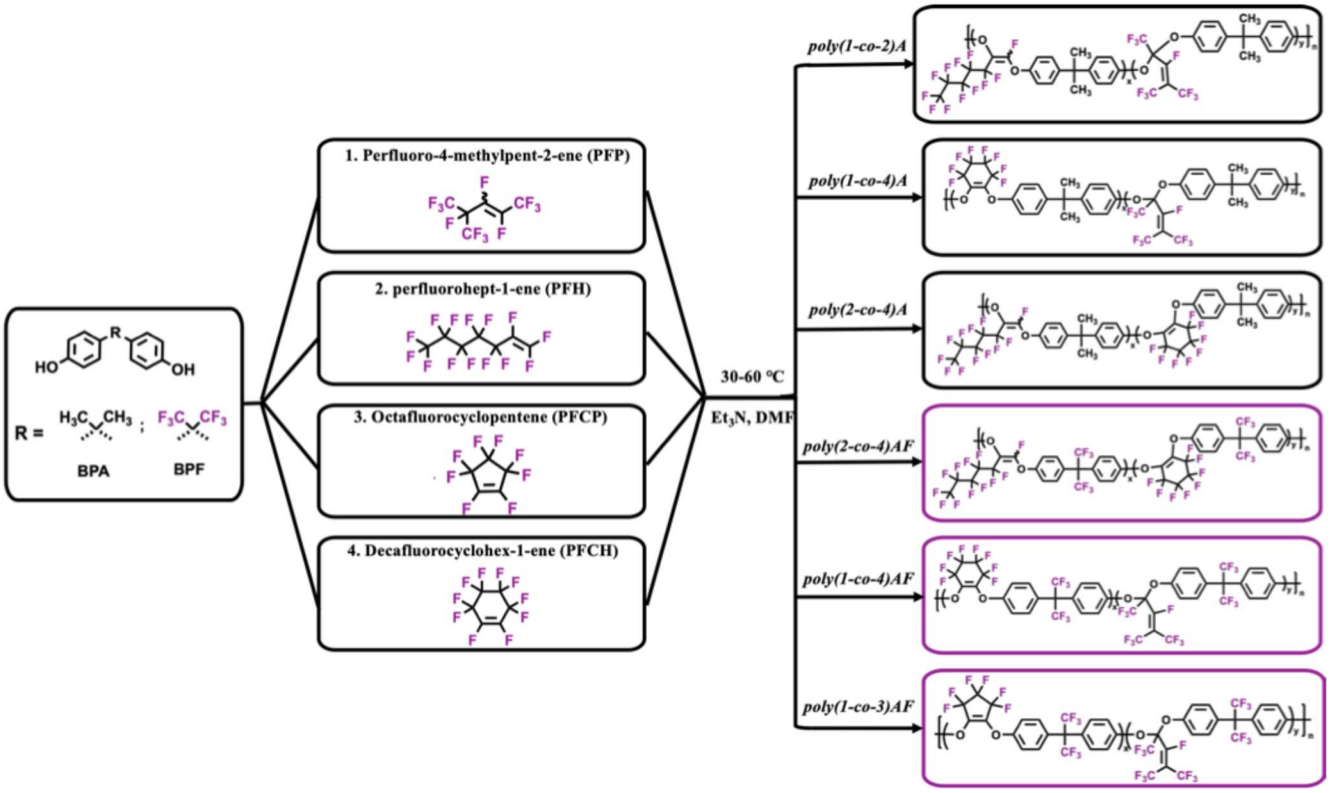
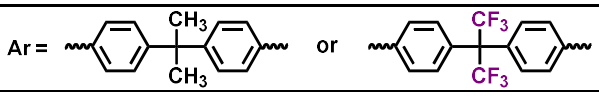
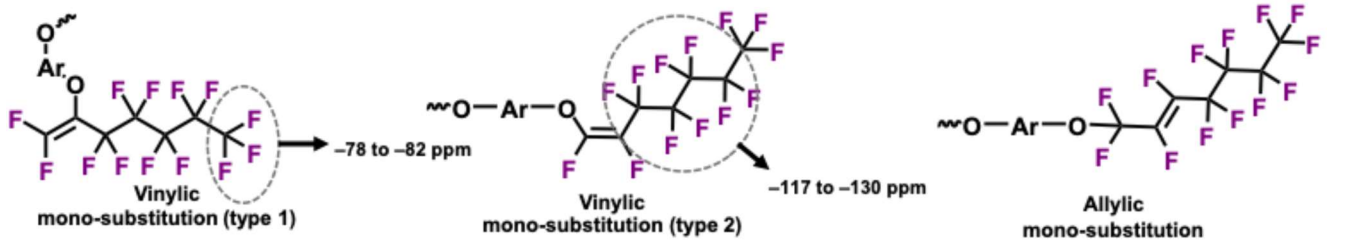
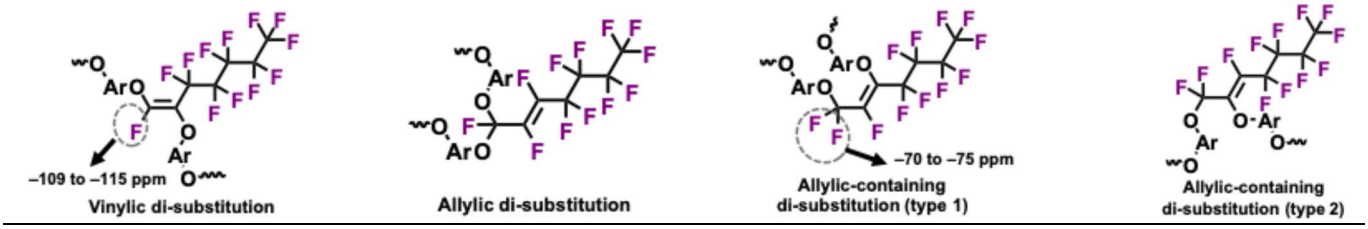
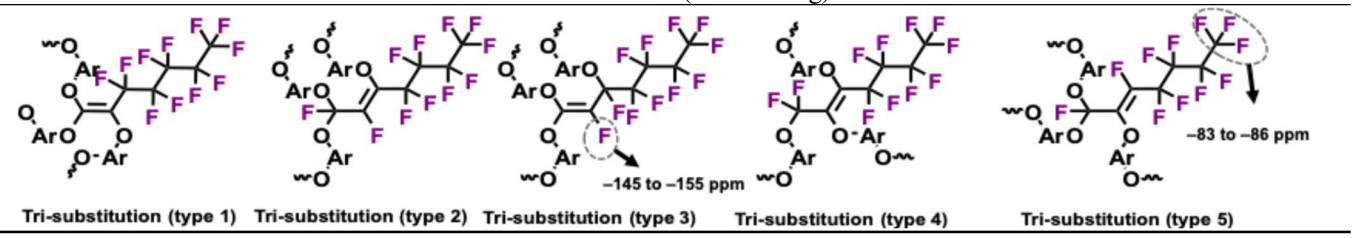


Figure 2. Step-growth copolymerization scheme of cyclic/acyclic perfluoroolefins with bisphenols.

The previously reported PFH addition reaction model provides diagnostic information for structural interpretation by ^{19}F NMR spectroscopy [16]. As summarized in Table 2, different PFH-derived substitution motifs give characteristic fluorine chemical-shift regions. Mono-substituted vinylic and allylic products, di-substituted structures associated with linear chain growth, and tri-substituted structures associated with branching or crosslinking each generate distinct fluorine environments [14]. Although the ^{19}F NMR spectra contain environments consistent with both vinylic and allylic substitution, substantial signal overlap prevents quantitative determination of the individual contributions of these pathways to branching and network formation.

Table 2. Representative PFH-derived substitution motifs and diagnostic ^{19}F NMR chemical-shift regions associated with mono-, di-, and tri-substituted products formed during bisphenol-based addition–elimination polymerization [14].

Outcomes from addition-elimination polymerization of perflourohept-1-ene with bisphenols. Ar = 
Mono-substitution

Di-substitution (linear chain growth)

Tri-substitution (crosslinking)


^{19}F NMR spectroscopy was used as the primary tool for assessing fluorinated environments attributable to the two feed components and estimating their relative proportions within the isolated THF-soluble fractions in all the perfluoroolefin-containing polymers reported here. PFP introduces branched acyclic fluorocarbon environments, and PFH contributes pendant and terminal perfluoroalkyl groups together with vinylic and allylic substitution motifs. From a steric standpoint, the more highly substituted PFP fluoroalkene is expected to be less accessible to initial phenoxide attack than the terminal fluoroalkene of PFH. However, overall polymerization behavior is governed by both steric accessibility and electronic/substitution effects. We previously found that PFP can react faster than PFH and exhibits a strong tendency toward tertiary substitution, branching, and gelation [14]. High free-volume PFCH and PFCP monomers introduce distinct cyclic fluorocarbon resonances. As this fluorine chemical shift can overlap and broaden in polymeric materials, the spectra were interpreted by comparing the observed resonances with expected chemical-shift regions for the parent perfluoroolefins.

Control of the reaction conditions is particularly critical in these mixed perfluoroolefin systems as the comonomers differ in electrophilicity, steric demand, and preferred substitution pathways. Stronger bases increase the equilibrium concentration of reactive phenoxide species and accelerate polymer formation. These faster rates also accelerate rapid tertiary substitution, premature branching, and gelation. Accordingly, triethylamine was selected to provide a more moderate basic environment and to better regulate the formation of insoluble products. In this work, Et_3N was used in DMF under anhydrous conditions at 30–60 °C, as shown in Figure 2.

Several initial screening reactions conducted for 24 h produced both THF-soluble and THF-insoluble fractions. consistent with continued tertiary addition–elimination reactions and progressive network

development. To obtain processable materials suitable for consistent solution-state characterization, the corresponding preparative reactions were repeated under otherwise identical conditions and terminated after 23 h. This earlier isolation generally favored recovery of the THF-soluble fraction and is treated as an empirical processing adjustment rather than a precisely established gel point. Preliminary time-point observations showed that the THF-soluble fraction isolated at 22 h had a lower M_n, whereas the 23 h material exhibited greater molar-mass development; further reaction increasingly favored formation of THF-insoluble material without significant molar mass change for the soluble fraction (Figure S22). Thus, 23 h was selected as a practical processing point for recovering a higher-molar-mass soluble fraction rather than as a kinetically defined reaction endpoint. The soluble fractions are attributed to linear or moderately branched copolymer precursors, whereas THF-insoluble fractions are consistent with more extensively branched or networked material. The formation of an insoluble network material is consistent with our previous study of related PFP/PFH–bisphenol systems, in which substantial gel fractions and crosslinked products were observed and characterized [14]. As the present study focuses on soluble, processable copolymers, the reported characterization herein was performed on the fully THF-soluble products obtained from the 23 h preparative reactions. Detailed characterization of the insoluble fractions, including quantitative gel-fraction analysis, will be the subject of a future report. Together, the spectroscopic, chromatographic, solubility, and thermal data provide a consistent framework for evaluating how perfluoroolefin structure, comonomer pairing, and bisphenol A/AF identity influence copolymer formation and material response.

*3.2. Copolymerization of PFP and PFH with Bisphenols [**Poly(1-co-2)A**]*

The copolymerization of perfluoro-4-methylpent-2-ene (PFP) and perfluorohept-1-ene (PFH) with bisphenol-A (BPA) was carried out under triethylamine-mediated addition–elimination conditions to give the soluble copolymer ***poly(1-co-2)A*** (Figure 2). This system was selected as the first mixed acyclic perfluoroolefin example because PFP and PFH differ substantially in structure and reaction rate. These structural differences are consistent with our previous observations that sterically hindered PFP readily undergoes nucleophilic addition and branching, whereas less substituted PFH exhibits greater reactivity under these conditions independent of bisphenols used [14]. It should be noted, however, that at lower temperatures (0–10 °C), PFP exhibits higher reactivity with bisphenols when it is the only olefin monomer present compared to bisphenol homopolymerization of PFH. Whereas fluoroolefin copolymerization of PFH and PFP with bisphenols without regard to temperature afforded copolymers with enriched PFH.

The ^{19}F NMR spectrum of ***poly(1-co-2)A*** (Figure S3) contains resonance patterns consistent with incorporation of both substituted PFP and substituted PFH units within the isolated soluble copolymer. Signals associated with PFP-derived fluorinated environments appear at −55.7 to −63.9 ppm, assigned to substituted CF_3 groups, and at −77.6 ppm, assigned to a substituted vinylic fluorine environment. A weak resonance at −70.4 ppm is attributed to an O−CF_2 environment. The PFH-derived terminal CF_3 groups appear between −80.9 and −86.6 ppm, while the broad signals from −111.0 to −127.5 ppm are assigned to adjacent CF_2 units along the fluorinated chain. Additional resonances at −106.6 and −154.2 ppm are consistent with substituted vinylic fluorine environments generated through the addition–elimination process. The broad and partially overlapping resonances reflect the presence of multiple vinylic, allylic, and more highly substituted fluorinated environments within the polymer. Integration of NMR signals, normalized for the number of fluorine nuclei represented by each signal, gave an estimated copolymer composition of approximately 77% PFH and 23% PFP for the isolated THF-soluble fraction. These results indicate preferential incorporation of PFH while confirming that PFP-derived units are retained within the soluble copolymer fraction. Olefin compositions are estimated from ^{19}F NMR integrations of the isolated THF-soluble fractions. The ^{1}H NMR spectrum displays the incorporation of the BPA-derived aromatic

component (Figure S2) through aromatic signals observed in the 6.6–7.2 ppm region, consistent with substituted phenylene. The isopropylidene methyl groups of BPA appear as a broadened signal near 1.5–1.7 ppm, confirming retention of the central bridging unit. Additional broadening across all regions reflects the polymeric nature of the material and the presence of multiple substitution environments. The ATR-FTIR spectrum is also provided in the Supporting Information (Figure S4) and shows the combined presence of fluorocarbon absorptions and aromatic/ether-associated bands. These features support the formation of semi-fluorinated polymeric material. GPC analysis of the THF-soluble ***poly(1-co-2)A*** fraction (Figure S5) showed a unimodal elution profile, suggesting that clearly separated polymer populations do not dominate the soluble material. Based on conventional polystyrene calibration, ***poly(1-co-2)A*** exhibited M_n = 13.2 kDa with a PDI of 1.3 (Table 1). These values should be interpreted as relative molecular masses because fluorinated copolymers and polystyrene standards have very different hydrodynamic volumes for equivalent molecular mass. The fluorinated polymers' molecular mass per unit chain length in solution could be substantially due to a small atomic radius and a 19-fold higher atomic weight than hydrogen. The GPC data confirm the formation of a measurable soluble polymer fraction with a comparatively narrow molecular-mass distribution.

Thermal stability for ***poly(1-co-2)A*** was evaluated by TGA, and DTG data under nitrogen and air (Figure S6), where 5% weight-loss temperatures ($T_{d5\%}$) of 262 °C and 379 °C, respectively, were measured (Table 1), demonstrating a pronounced atmosphere-dependent thermal response. Both measurements were obtained under the same heating rate and controlled gas-flow conditions. DSC analysis of ***poly(1-co-2)A*** (Figure S7) showed a glass-transition temperature of 114 °C (Table 1), consistent with an amorphous semi-fluorinated copolymer containing both rigid BPA-derived aromatic segments and flexible fluorinated comonomer units. An irreversible exothermic event was observed during the first heating cycle (from 133–189 °C, with the highest heat generation at 165 °C). This event was absent in the subsequent scans, demonstrating an irreversible thermally activated crosslinking. This behavior is consistent with thermally induced crosslinking through residual reactive fluoroalkene sites.

A film obtained from the soluble ***poly(1-co-2)A*** fraction is shown in Figure 3. The ability of ***poly(1-co-2)A*** to form a continuous film after THF evaporation indicates that the soluble fraction has sufficient cohesion and processability, distinguishing it from crosslinked insoluble material.



Figure 3. Film formation of ***poly(1-co-2)A***.

*3.3. Copolymerization of PFP and PFCH with Bisphenols [**Poly(1-co-4)A/AF**]*

The copolymerization of perfluoro-4-methylpent-2-ene (PFP) and perfluorocyclohexene (PFCH) was examined with BPA and BPF to evaluate how bisphenol identity influences the incorporation of an acyclic perfluoroolefin with a cyclic perfluoroolefin. Based on ^{19}F NMR integration, the BPA-based copolymer ***poly(1-co-4)A*** contained 59% PFP and 41% PFCH, whereas the BPF-based copolymer ***poly(1-co-4)AF*** contained 35% PFP and 65% PFCH. These compositions indicate that both comonomers participate in the addition–elimination process, although the relative incorporation is strongly affected by the bisphenol structure.

The ^{19}F NMR spectra of ***poly(1-co-4)A*** and ***poly(1-co-4)AF*** are shown in Figure S9. ***poly(1-co-4)A,*** exhibited resonances attributable to PFP-derived fluorinated environments in the approximately −55.1 to

−83.2 ppm region and PFCH-derived fluorine environments from approximately −105.2 to −136.4 ppm. Weaker signals between approximately −140.0 and −155.0 ppm are consistent with substituted vinylic fluorine environments formed during addition–elimination polymerization. For ***poly(1-co-4)AF***, PFP-derived resonances appear near −55 to −60 ppm and −73.3 to −83.1 ppm, while the BPF CF_3 resonance near −64.2 ppm overlaps with the other CF_3 geminal groups in this region. PFCH fluorine signals within the ring structure are observed broadly from approximately −106.7 to −133.4 ppm, with additional substituted vinylic fluorine resonances near −151.2 to −154.5 ppm. The ^{1}H NMR spectrum of ***poly(1-co-4)A*** is provided in Figure S8 and confirms BPA incorporation through aromatic proton signals and the characteristic isopropylidene methyl resonance. ATR-FTIR spectra of ***poly(1-co-4)A*** and ***poly(1-co-4)AF*** are shown in Figure S10. Both copolymers display aromatic and ether-associated absorptions from the bisphenol component, together with strong fluorocarbon bands across the C–F stretching region, particularly between approximately 1300 and 1000 cm^{-1}. Additional absorptions below 1000 cm^{-1}, particularly in the 800–890 cm^{-1} region, are attributed to fluorinated cyclic units, and the region 920–980 cm^{-1} in the acyclic environments. These FTIR results support the formation of semi-fluorinated copolymer products.

GPC analyses of ***poly(1-co-4)A*** and ***poly(1-co-4)AF*** are provided (Figure S11). ***poly(1-co-4)A*** had a M_n = 13.1 kDa and a PDI = 1.9, while ***poly(1-co-4)AF*** exhibited M_n = 16.2 kDa and PDI = 1.1. The PDI observed for ***poly(1-co-4)A*** suggests a less controlled polymer growth process, likely arising from differences in reactivity between PFP and PFCH in the presence of BPA. Thermal analysis further distinguishes the two systems. ***poly(1-co-4)A*** exhibited T_g = 125 °C and $T_{d5\%}$ values of 244.0 °C under N_2 and 366.0 °C in air, whereas ***poly(1-co-4)AF*** exhibited T_g = 123 °C and higher $T_{d5\%}$ values of 409.0 °C under N_2 and 397.0 °C in air in (Table 1). Both copolymers display similar glass transition temperatures, indicating that segmental mobility is governed primarily by the aromatic backbone rather than fluorine content. The markedly higher thermal stability of ***poly(1-co-4)AF*** reflects a fundamental difference in chemical robustness. The combination of the 6F group in BPF and the greater PFCH incorporation increases the overall strong C–F bond density and reduces the number of thermally labile sites, thereby suppressing chain scission pathways. In contrast, the lower fluorine content and higher proportion of PFP-derived units in ***poly(1-co-4)A*** could introduce more reactive environments that initiate earlier degradation. These results demonstrate that fluorine content and monomer structure selection strongly influence thermal stability, even when glass-transition behavior remains largely unchanged. The TGA, DTG, and DSC data are shown in the supporting information (Figures S12 and S13), respectively.

*3.4. Copolymerization of PFH and PFCH with Bisphenols [**Poly(2-co-4)A/AF**]*

The copolymerization of PFH and PFCH was examined with BPA and BPF to evaluate the effect of bisphenol structure on systems containing one linear acyclic and one cyclic perfluoroolefin. Based on ^{19}F NMR integration, the BPA-based copolymer ***poly(2-co-4)A*** contained 57% PFH and 43% PFCH, whereas the BPF-based copolymer ***poly(2-co-4)AF*** contained 47% PFH and 53% PFCH under the same conditions. These compositions support the incorporation of both comonomers and indicate that BPF slightly favors higher PFCH incorporation for this pair.

The ^{19}F NMR spectra of ***poly(2-co-4)A*** and ***poly(2-co-4)AF*** are shown in Figure 4. Both spectra exhibit PFH-derived terminal CF_3 resonances at approximately −79.1 to −86.3 ppm, together with overlapping PFH- and PFCH-derived CF_2 signals between approximately −115.2 and −134.4 ppm. Weaker resonances near −110.1 ppm and within the −140.3 to −156.6 ppm region are consistent with substituted vinylic fluorine environments formed during addition–elimination polymerization. ***Poly(2-co-4)AF*** additionally displays the characteristic BPF-derived CF_3 resonance near −64.2 ppm. Together, these spectra support the presence of fluorinated environments derived from both PFH and PFCH in the isolated polymeric fractions.

The ^{1}H NMR spectrum of ***poly(2-co-4)A*** is provided in (Figure S14) and supports BPA incorporation through aromatic proton signals and the characteristic isopropylidene group peak.

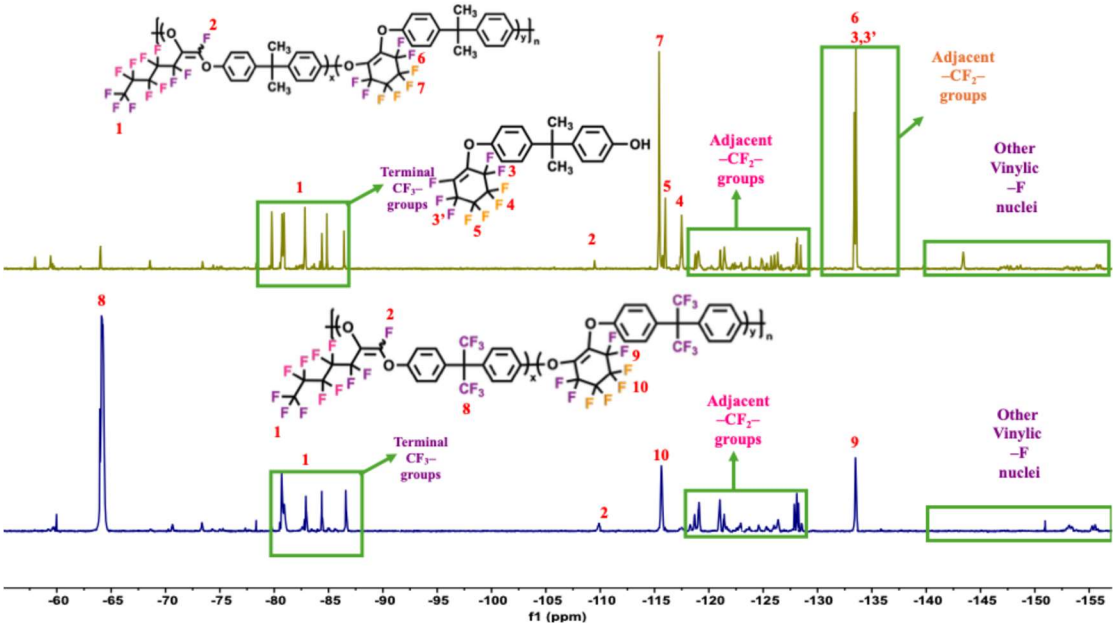
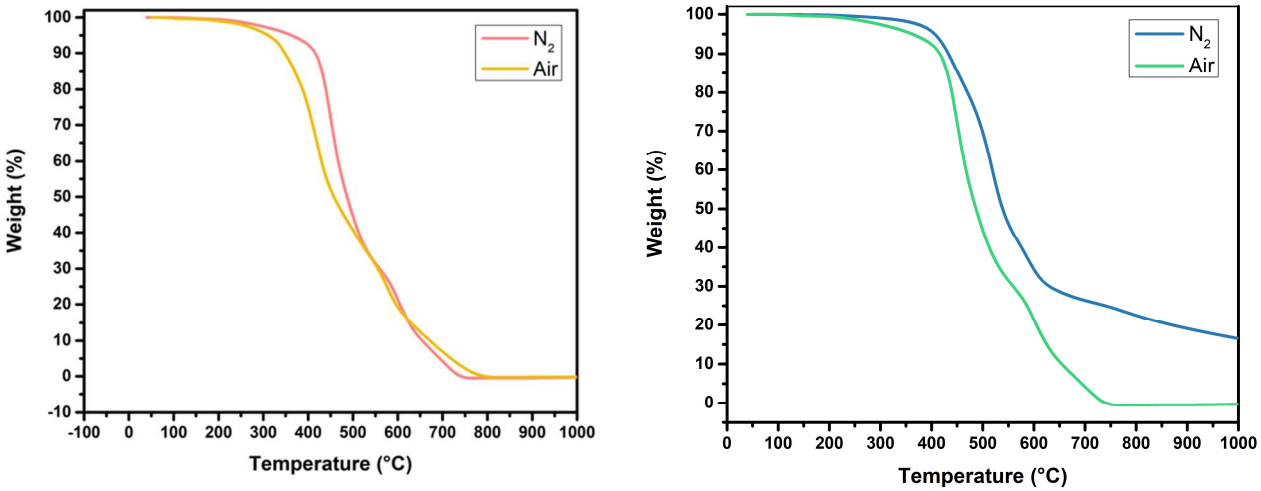


Figure 4. ^{19}F NMR (470 MHz, $CDCl_3$) analysis of copolymers ***poly(2-co-4)A*** (**top**), and ***poly(2-co-4)AF*** (**bottom**).

ATR-FTIR spectra of ***poly(2-co-4)A*** and ***poly(2-co-4)AF*** are shown in Figure S15. Both copolymers exhibit aromatic and ether-related transmittances from the bisphenol component, together with strong fluorocarbon bands in the C–F stretching region, especially between approximately 1300 and 1000 cm^{-1}. Additional absorptions below 1000 cm^{-1} are consistent with the 800–890 cm^{-1} region cyclic fluorocarbon and 900–950 cm^{-1} substituted acyclic fluoroolefin units. The IR data support the formation of PFH/PFCH copolymers.

GPC data provided in (Figure S16) for ***poly(2-co-4)A*** showed M_n = 15.2 kDa, and PDI = 1.1, while ***poly(2-co-4)AF*** showed M_n = 13.4 kDa, and PDI = 1.5. Thermal analysis showed a stronger bisphenol effect: ***poly(2-co-4)A*** exhibited T_g = 131 °C with $T_{d5\%}$ values of 363.0 °C under N_2 and 311 °C in air, whereas ***poly(2-co-4)AF*** exhibited a higher T_g = 201 °C and higher nitrogen stability with $T_{d5\%}$ = 406 °C, but lower stability with $T_{d5\%}$ = 363 °C in air. The TGA, DTG, and DSC data are shown in Figures 5 and 6, respectively. These results indicate that incorporating the BPF-derived segment increases chain rigidity and enhances thermal resistance in both nitrogen and air atmospheres, while also shifting the curing-related DSC response to a higher temperature range.



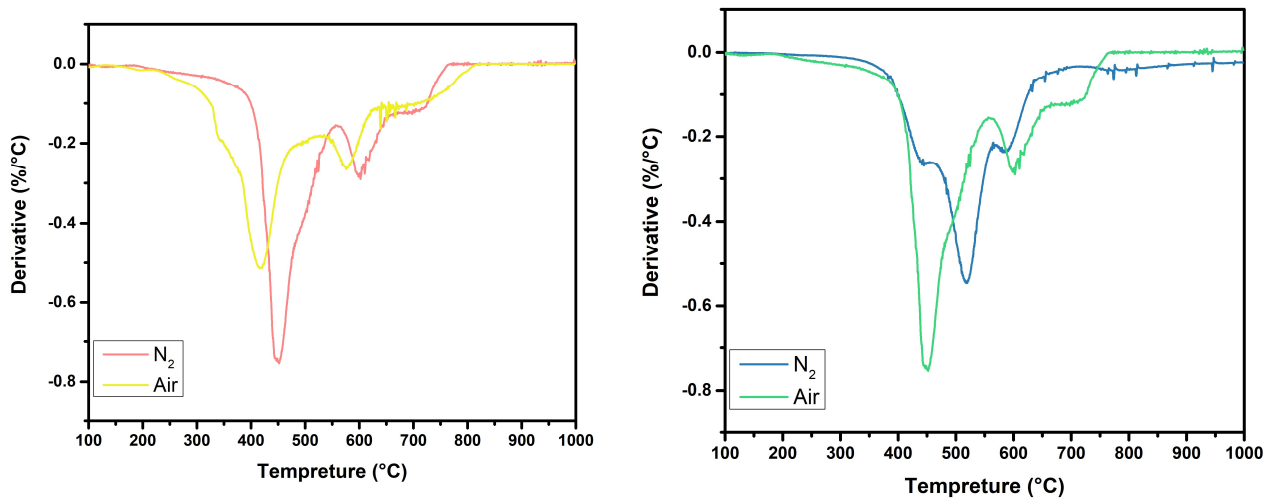


Figure 5. TGA (10 °C/min) of ***poly(2-co-4)A*** (**Top-Left**) and ***poly(2-co-4)AF*** (**Top-Right**), DTG of ***poly(2-co-4)A*** (**Bottom-Left**) and ***poly(2-co-4)AF*** (**Bottom-Right**).

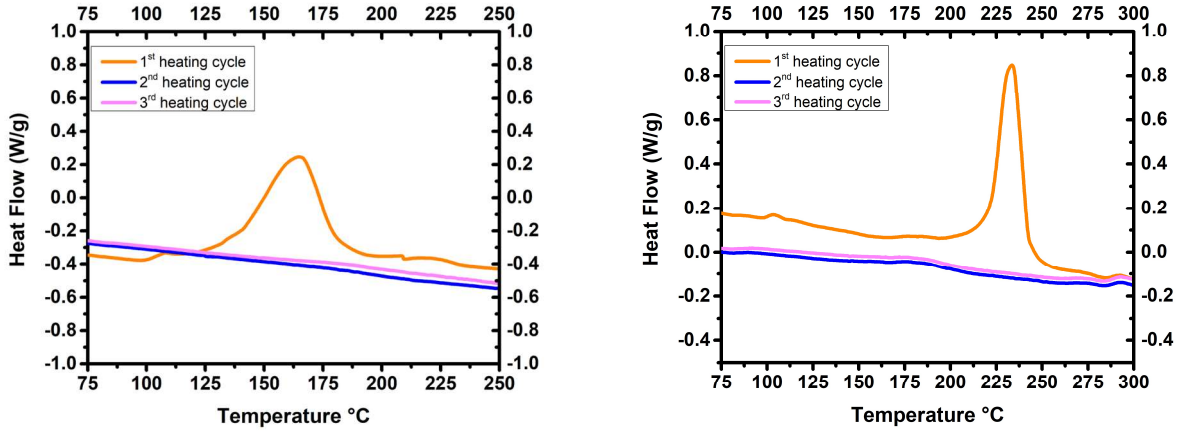


Figure 6. DSC analysis (10 °C/min in N_2) of ***poly(2-co-4)A*** (**Left**) and ***poly(2-co-4)AF*** (**Right**).

*3.5. Copolymerization of PFP and PFCP with Bisphenol-AF[**poly(1-co-3)AF**]*

The copolymerization of PFP and PFCP with BPF was examined to evaluate the compatibility of a branched acyclic perfluoroolefin with a highly reactive cyclic perfluoroolefin. ^{19}F NMR integration estimated that ***poly(1-co-3)AF*** contained 34% PFP and 66% PFCP, indicating preferential incorporation of the cyclic PFCP comonomer by addition–elimination. The ^{19}F NMR spectrum of ***poly(1-co-3)AF*** is shown in Figure S17. Signals between −59.4 and −86.1 ppm are attributed to PFP-derived, with the intense BPF-derived CF_3 signal near −64.5 ppm overlapping this region. PFCP-derived cyclic fluorine resonances are observed primarily between approximately −110.0 and −134.4 ppm, while weaker signals from approximately −140.0 to −151.1 ppm are consistent with substituted vinylic fluorine environments. The spectrum contained fluorinated environments attributable to both PFP and PFCP. ATR-FTIR spectra are provided in (Figure S18) and further support the formation of the semi-fluorinated copolymer. ***poly(1-co-3)AF*** displays aromatic and ether-associated absorptions from the BPF segment together with strong fluorocarbon bands across the C–F stretching region, particularly between approximately 1300 and 1000 cm^{-1}. Additional absorptions below 1000 cm^{-1} are consistent with 800–890 cm^{-1} cyclic fluorocarbon and substituted 900–960 cm^{-1} acyclic fluoroolefin structures. As in the other copolymer systems, IR supports polymer formation but does not independently resolve comonomer sequence or substitution pathway. GPC analysis is shown in Figure S19. ***Poly(1-co-3)AF*** exhibited M_n = 13.0 kDa, and PDI = 1.3. Thermal analysis

showcased that ***poly(1-co-3)AF*** had the T_g in the series at 116 °C, consistent with the combined rigidity of PFCP and BPF units. TGA, and DTG data in (Figure S20) showed high thermal stability, with $T_{d5\%}$ values of 418 °C under N_2 and 395 °C in air. The DSC thermogram (Figure S21) further supports a thermally robust material response. The ***poly(1-co-3)AF*** data demonstrate that PFP and PFCP can be combined through addition–elimination copolymerization to produce a PFCP-rich semi-fluorinated copolymer with high glass-transition temperature and high thermal stability.

4. Conclusions

A range of unsaturated semi-fluorinated copolymers was synthesized via addition–elimination copolymerization of cyclic and acyclic perfluoroolefins with BPA or BPF to produce THF-soluble semi-fluorinated copolymers with defined unsaturation for subsequent reaction. NMR integration provided estimated olefin ratios in the copolymers vs. the consistent 1:1 molar olefin monomer feed. GPC established the relative molar masses, while DSC and TGA provided thermal characterization of the copolymers. ^{19}F NMR spectra and GPC exhibited that the resulting products were random copolymers rather than physical mixtures of different homopolymers. Among the copolymer series, structure–property relationships depended on both perfluoroolefin pairing and bisphenol identity. In general, great differences in cyclic *vs.* acyclic olefin reactivity were not observed under these conditions. The influence of bisphenol was system dependent. The BPA- and BPF-based copolymers exhibited similar glass-transition temperatures, but all of the BPF-containing polymer products presented substantially greater thermal stability. In the PFH/PFCH system, BPF incorporation increased both the glass-transition temperature and thermal stability under inert and air conditions. ***Poly(2-co-4)AF*** exhibited the highest T_g of the series at 201 °C, whereas the PFCP-rich copolymer displayed the highest $T_{d5\%}$ under nitrogen at 418 °C. These findings illustrate that thermal performance reflects the combined effects of fluoroolefin and bisphenol structures, copolymer composition, and the extent of thermally induced branching and network development during the thermal analysis experiments rather than fluorine content alone. This combination of processable polymers provides access to soluble linear-to-branched precursors that retain residual unsaturation and can undergo further formulation and crosslinking to thermoset products such as valuable fluoroelastomers. Future studies will focus on network formation from blends of commercial polymers such as PVDF, their properties, and applications such as coatings and membranes.

Supplementary Materials

The following supporting information can be found at: https://www.sciepublish.com/article/pii/1256, Figures S1–S22 include reaction mechanisms, NMR spectra, ATR-FTIR spectra, idealized structures, Thermal Analysis Characterizations and GPC traces for ***poly(x-co-y)A/AF***.

Statement of the Use of Generative AI and AI-Assisted Technologies in the Writing Process

During the preparation of this manuscript, the authors used ChatGPT (OpenAI) to improve language, clarity, and readability. After using this tool, the authors reviewed and edited the content and take full responsibility for the content of the published article.

Acknowledgments

The authors would like to acknowledge the Department of Chemistry, Mississippi State University, and the Helium recovery system the NSF Award 2304919, and MRI (NSF award 2215258) and CHE/MCB 2304919, for supporting this project.

Author Contributions

E.M.: Writing—original draft, Writing—review & editing, Visualization, Validation, Resources, Project administration, Methodology, Investigation, Formal analysis, Data curation, Conceptualization. M.E.S.: Writing—review & editing, Validation, Investigation, Conceptualization. G.M.: Writing—review & editing, Validation, Conceptualization. W.W.J.: Writing—review & editing, Formal analysis, Investigation. E.J.: Investigation, Formal analysis. G.O.M.O.: Investigation. C.U.P.J.: Writing—review & editing, Validation, Supervision, Methodology, Conceptualization. D.W.S.J.: Writing—review & editing, Validation, Supervision, Resources, Project administration, Methodology, Funding acquisition, Conceptualization.

Ethics Statement

Not applicable. This study did not involve human participants, animals, clinical samples, or any research activity requiring ethical approval.

Informed Consent Statement

Not applicable. This study did not involve human participants.

Data Availability Statement

The data supporting the findings of this study are available within the article and its Supporting Information. Additional raw data is available from the corresponding author upon reasonable request.

Funding

This research was supported by HAND Technologies Inc. through the purchase and provision of chemicals and research materials. No grant number was assigned.

Declaration of Competing Interest

The authors declare that they have no known competing financial interests or personal relationships that could have appeared to influence the work reported in this paper.

References

1. Smith DW, Jr., Iacono ST, Iyer SS. (Eds.) *Handbook of Fluoropolymer Science and Technology*, 1st ed.; John Wiley & Sons, Inc.: Hoboken, NJ, USA, 2014. DOI:10.1002/9781118850220
2. Ameduri B, Boutevin B. Chapter 3—Synthesis, properties and applications of fluoroalternated copolymers. In *Well-Architectured Fluoropolymers: Synthesis, Properties and Applications*; Elsevier Science: Amsterdam, The Netherlands, 2004; pp. 187–230. DOI:10.1016/B978-008044388-1/50012-1
3. Gardiner J. Fluoropolymers: Origin, Production, and Industrial and Commercial Applications. *Aust. J. Chem.* **2014**, *68*, 13–22. DOI:10.1071/CH14165
4. Církva V, Paleta O, Ameduri B, Boutevin B. Radical additions to fluoroolefins. Thermal reaction of perfluoroallyl chloride with perfluoroalkyl iodides as a selective synthesis of terminal perfluoroolefins. *J. Fluor. Chem.* **1995**, *75*, 87–92. DOI:10.1016/0022-1139(95)03202-O
5. Mortazavian S, Hooper J, Absallout I, Hofmann R. Granular Activated Carbon for PFAS Removal in Municipal Wastewater: A Rapid Small-Scale Column Test Study. *ACS EST Water* **2025**, *5*, 2145–2154. DOI:10.1021/acsestwater.4c00919
6. Wu J, Xi Y, McCandless GT, Xie Y, Menon R, Patel Y, et al. Synthesis and Characterization of Partially Fluorinated Polybenzoxazine Resins Utilizing Octafluorocyclopentene as a Versatile Building Block. *Macromolecules* **2015**, *48*, 6087–6095. DOI:10.1021/acs.macromol.5b01014
7. Améduri B. The Promising Future of Fluoropolymers. *Macromol. Chem. Phys.* **2020**, *221*, 1900573. DOI:10.1002/macp.201900573

8. Dolui S, Kumar D, Banerjee S, Ameduri B. Well-Defined Fluorinated Copolymers: Current Status and Future Perspectives. *Acc. Mater. Res.* **2021**, *2*, 242–251. DOI:10.1021/accountsmr.1c00015
9. Crone BC, Speth TF, Wahman DG, Smith SJ, Abulikemu G, Kleiner EJ, et al. Occurrence of per- and polyfluoroalkyl substances (PFAS) in source water and their treatment in drinking water. *Crit. Rev. Environ. Sci. Technol.* **2019**, *49*, 2359–2396. DOI:10.1080/10643389.2019.1614848
10. Geng N, Lu C, Li W, Liu Q, Zhou Z, Yang T, et al. Fluoro-Functionalized Polyether Electrolytes Enabling High-Energy-Density Solid-State Lithium-Metal Batteries. *ENERGY Environ. Mater.* **2026**, *9*, e70188. DOI:10.1002/eem2.70188
11. Malik AA, Sharts CM, Shellhamer DF. Perfluoroalkenyl ethers of simple sterols. *J. Fluor. Chem.* **1987**, *34*, 409–420. DOI:10.1016/S0022-1139(00)85183-0
12. Narayanan G, Faradizaji B, Mukeba KM, Shelar KE, Silva MD, Patrick A, et al. Perfluorocyclohexenyl (PFCH) aromatic ether polymers from perfluorocyclohexene and polycyclic aromatic bisphenols. *Polym. Chem.* **2020**, *11*, 5051–5056. DOI:10.1039/D0PY00569J
13. Muñoz G, Chamberlain KM, Athukorale S, Ma G, Gu X, Pittman CU, Jr., et al. Teaching Old Polymers New Tricks: Improved Synthesis and Anomalous Crystallinity for a Lost Semi-Fluorinated Polyaryl Ether via Interfacial Polymerization of Hexafluoroacetone Hydrate and Diphenyl Ether. *Macromol. Rapid Commun.* **2023**, *44*, 2200737. DOI:10.1002/marc.202200737
14. Solovyev ME, Muñoz G, Masaeli E, Pittman CU, Jr., Smith DW, Jr. Polycondensation of model perfluoroolefins with bisphenols toward upcycling of perfluoroalkyl substances (PFAS). *J. Fluor. Chem.* **2026**, *292*, 110572. DOI:10.1016/j.jfluchem.2026.110572
15. Muñoz G, Chamberlain KM, Solovyev ME, Smith DW, Jr., Pittman CU, Jr. Electrophilic Routes to 6F Polymers and Attempted Synthesis of Semi-fluorinated Group IVB Metallocene Polymers. *J. Inorg. Organomet. Polym. Mater.* **2024**, *34*, 2834–2854. DOI:10.1007/s10904-024-03031-5
16. Groβ U, Storek W. Reaktionen von fluoralkenen I. Zur nucleophilen reaktion von F-hept-1-en mit alkoholen. *J. Fluor. Chem.* **1984**, *26*, 457–465. DOI:10.1016/S0022-1139(00)80973-2
17. Krishnan R, Parthiban A. A multifunctionalization of octafluorocyclopentene under mild conditions. *Eur. Polym. J.* **2018**, *101*, 66–76. DOI:10.1016/j.eurpolymj.2018.01.024
18. Alvino EL, Lochmaier EC, Iacono ST, Jennings AR. Chemoselective nucleophilic additions to perfluorocyclopentene: An efficient building block to highly fluorinated molecules. *J. Fluor. Chem.* **2020**, *232*, 109454. DOI:10.1016/j.jfluchem.2020.109454
19. Ok S, Hartmann B, Duran H, Eickmeier H, Haase M, Scheler U, et al. Correlations between microstructure and crystallization of the fluorinated terpolymer of tetrafluoroethylene, hexafluoropropylene, and vinylidene fluoride. *J. Polym. Sci. Part B Polym. Phys.* **2019**, *57*, 1402–1408. DOI:10.1002/polb.24886
20. Endo K, Yamade T. Synthesis and Characterization of Polymers from Bisphenol Derivatives and Perfluorinated Aromatic Compounds. *Polym. J.* **2008**, *40*, 212–216. DOI:10.1295/polymj.PJ2007168
21. Iacono ST, Budy SM, Ewald D, Smith DW, Jr. Facile preparation of fluorovinylene aryl ether telechelic polymers with dual functionality for thermal chain extension and tandem crosslinking. *Chem. Commun.* **2006**, *42*, 4844–4846. DOI:10.1039/B610157G
22. Shelar KE, Mukeba KM, Mills K, Smith DW, Jr. Renewable isosorbide-enchained semi-fluorinated aromatic ether polymers. *J. Polym. Sci.* **2022**, *60*, 2500–2507. DOI:10.1002/pol.20220161
23. Mukeba KM, Faradizaji B, Shelar KE, Pittman CU, Jr., Smith DW, Jr. Semi–fluorinated arylene vinylene ether (FAVE) telechelic polymers from polycyclic aromatic hydrocarbon bisphenols and trifluorovinyl aryl ethers. *Polymer* **2020**, *209*, 122955. DOI:10.1016/j.polymer.2020.122955
24. Sharma B, VanDerveer DG, Liff SM, Smith DW, Jr. Bis-perfluorocycloalkenyl (PFCA) aryl ether monomers towards a versatile class of semi-fluorinated aryl ether polymers. *Tetrahedron Lett.* **2013**, *54*, 3609–3612. DOI:10.1016/j.tetlet.2013.04.087
25. Smith DW, Jr., Babb DA. Perfluorocyclobutane Aromatic Polyethers. Synthesis and Characterization of New Siloxane-Containing Fluoropolymers. *Macromolecules* **1996**, *29*, 852–860. DOI:10.1021/ma951149b
26. Shelar KE, Le N, Mukeba KM, Dey S, Farajidizaji B, Athukorale S, et al. Triphenylene containing blue-light emitting semi-fluorinated aryl ether polymers with excellent thermal and photostability. *Mater. Chem. Front.* **2022**, *6*, 1391–1404. DOI:10.1039/D2QM00099G
27. Parthiban A, Ranganathan K. Octafluorocyclopentene—A versatile tetrafunctional monomer for making tunable, high surface area, microporous ladder polymers. *J. Fluor. Chem.* **2016**, *191*, 70–76. DOI:10.1016/j.jfluchem.2016.09.013

28. Sharma B, Faisal M, Liff SM, Smith DW, Jr. Triarylamine-enchained semifluorinated perfluorocycloalkenyl (PFCA) aryl ether polymers. *Appl. Petrochem. Res.* **2015**, *5*, 35–45. DOI:10.1007/s13203-014-0063-0
29. Mukeba KM, Shelar KE, Faradizaji B, Caldona EB, Pittman CU, Jr., Smith DW, Jr. Semi-fluorinated Poly(aryl ether sulfone)s via step-growth polymerization of perfluorocyclohexene with bisphenols. *Polymer* **2022**, *253*, 124937. DOI:10.1016/j.polymer.2022.124937
30. Muñoz G, Chamberlain KM, Athukorale S, Pittman CU, Jr., Smith DW, Jr. Semi-fluorinated (6F) polyaryl ethers and polyphenylenes via interfacial electrophilic condensation polymerization with hexafluoroacetone hydrate. *Polymer* **2024**, *293*, 126642. DOI:10.1016/j.polymer.2023.126642
31. Dmowski W. Nucleophilic reactions of fluoroolefins. I. Reactions of 1-(2-tetrahydrofuryl)-pentafluoropropene with alkoxide ions. *J. Fluor. Chem.* **1980**, *15*, 299–313. DOI:10.1016/S0022-1139(00)81465-7
32. Murray CB. New Methodology for Nucleophilic Fluorination. Ph.D. Thesis, Durham University, Durham, UK, 2003.